Jurnal Teknologi

Full Paper

SEISMIC FRAGILITY OF INFILLED STEEL BUILDINGS WITH CHEVRON AND X-BRACED CONFIGURATIONS

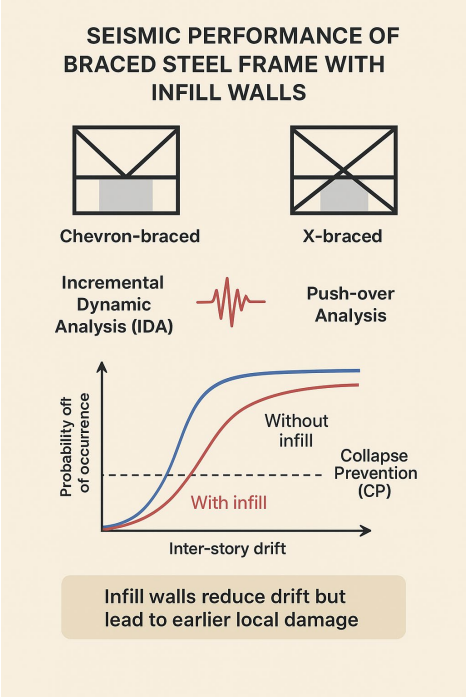
Mohammed Mustafa Hussein Al-Amrani[a]*, Salihi Salihi Abdu[a], Mohammadreza Vafaei[b], Sohpia C. Alih[a], Vigh László Gergely[a]

[a]Department of Structural Engineering, Faculty of Civil Engineering, Budapest University of Technology and Economics, Műegyetem rakpart 3, Budapest 1111 Hungary
[b]Department of Structures and Materials, Faculty of Civil Engineering, Universiti Teknologi Malaysia, 81310 Johor Bahru, Johor, Malaysia

Article history
Received
29th November 2025
Received in revised form
5th February 2026
Accepted
11th February 2026
Published
1st November 2026

*Corresponding author
alamranimoh@edu.bme.hu

Graphical abstract



Abstract

The use of bracing frames to resist lateral forces in high seismic regions is essential, as earthquakes can cause severe structural damage and loss of life. This study investigates the interaction between chevron and X-braced steel frames and infill walls, focusing on their seismic fragility. The main objective is to develop and assess fragility curves for twelve two-dimensional structural models subjected to seismic loading. Incremental Dynamic Analysis (IDA) and Push-over Analysis were employed using fifteen ground motion records in SAP2000 to evaluate failure modes, inter-story drift demands, and fragility behavior for models with and without infill walls. Results from the pushover analysis indicate that in concentric braced frames, the initial damage state appears earlier in models with infill walls, while frames without infill experience this state at higher drift levels. Conversely, IDA results reveal that frames without infill walls exhibit greater inter-story drift demands and higher overall capacity than those with infill walls. This suggests that while infill walls contribute to stiffness and reduce drift, they also lead to earlier onset of local damage. Fragility curves developed through statistical analysis demonstrate that two- and three-story frames without infill have a higher probability of reaching the Collapse Prevention (CP) performance level compared to those with infill. However, for taller frames (four to seven stories), the opposite trend is observed. These findings emphasize the complex influence of infill walls on the seismic performance of braced steel structures and provide valuable insights for safer structural design in earthquake-prone regions.

Keywords: Chevron braced frames, X-braced frames, Infill wall, Incremental Dynamic - Push-over Analysis, Fragility curves, Peak ground acceleration.

1.0 INTRODUCTION

Infill walls and braced frames represent integral structural elements within building design, strategically employed to augment seismic resilience and avert the structural collapse of edifices during seismic events. Together, they synergize to confer augmented structural robustness by adroitly addressing various facets of structural performance. Empirical investigations conducted during prior seismic occurrences consistently underscore the substantial merits accorded by infill walls in steel

DOI: https://doi.org/10.11113/jurnalteknologi.v88.26026

frames structures. These merits encompass heightened energy dissipation, augmented stiffness, and fortified strength. However, it is imperative to recognize the dual effect exerted by infill walls on structural seismic response, encompassing both beneficial and adverse effects. On a positive note, they furnish augmented energy dissipation and enhanced structural robustness. Yet their inclusion may introduce complexities by engendering irregularities or adverse local interactions with framing components. Hence, a comprehensive comprehension of their dynamic implications on structural systems assumes paramount significance for efficacious seismic design and analysis. The evaluation of the seismic performance of braced frames in historical seismic events typically involves the scrutiny of the structural response exhibited by buildings and edifices incorporating such systems during seismic occurrences. Seismic events often cause severe damage to structures, leading to loss of life. Truss frames are crucial for enhancing structural resilience, but failures have occurred, particularly due to the complex interaction between infill walls and abutment frames. Despite being commonly used for lateral resistance, truss frames are often designed without accounting for the impact of infill walls, which can significantly influence seismic performance. [1].

Fragility curves are essential for assessing potential damage to structural and non-structural elements of a building due to ground motion-induced vibrations. Over the past several decades, significant efforts have been made by researchers to develop seismic fragility curves for various types of braced frames. The Applied Technology Council (ATC) has recently developed drift-based fragility curves to categorize earthquake-induced damage in steel plate shear walls and steel frames. [2]. A recent study assessed the seismic performance of Eurocode-8 compliant concentrically braced steel frames with chevron braces and replaceable hourglass-shaped duplex stainless-steel pins. These pins were designed to enhance post-yield stiffness and reduce residual drifts after earthquakes, ensuring that inter-storey drifts stayed below the 1/300 threshold. The study also developed damage accumulation prediction models, with the cumulative absolute velocity-based model proving to be the most effective. M. Hassan et al. & Ali Mohammadgholipour et al. investigated the seismic performance of 6-story Chevron-braced steel frames (CBSFs) designed using PBPD under mainshock and mainshock-aftershock sequences. A new PBPD method incorporating aftershock effects was proposed, and fragility curves were developed to compare the seismic vulnerability of frames designed with the original and proposed methods across various damage states (Immediate Occupancy, Life Safety and Collapse Prevention). [5] studied the seismic performance of reinforced concrete structures retrofitted with steel braces, finding that V-braced frames offer superior resilience compared to K-braced frame which two diagonal members connect to a column at approximately mid-height, forming a shape similar to the letter K and D-braced frame (also known as a Diagonal braced frame) which consists of a single diagonal member extending from one beam–column joint to the opposite joint within the same bay, forming a "D-shaped" load path. The collapse fragility analysis reveals that various frame types have different likelihoods of collapsing during seismic events, highlighting the importance of enhancing design strategies. [6] The fragility curves provide a valuable tool for estimating earthquake-induced losses and informing post-earthquake rehabilitation strategies. [7] [8] explored seismic fragility analysis and incremental dynamic analysis (IDA) to assess the vulnerability of reinforced concrete structures. The results indicate that updated design standards and fragility curves, which evaluate the probability of exceeding different performance levels, enhance the seismic performance of braced frames compared to older standards. [9] studied the seismic performance of special concentric braced frames with 2, 4, and 6-story structures under various frequency contents by simulating 60 earthquake records and Incremental Dynamic Analysis (IDA) to develop IDA and fragility curves, emphasizing the importance of frequency content in creating effective seismic fragility curves. Fragility curves were developed by [10] using experimental data to evaluate the damage states of CBFs with square HSS braces subjected to earthquake ground motions. The likelihood of brace fracture for designs following seismic provisions was found to be as high as 85% under anticipated inelastic performance levels. Another study by [11] introduces single and dual-parameter fragility curves for four steel brace types in CBFs, emphasizing the role of SDR in estimating damage probabilities. It underscores the significance of accounting for epistemic uncertainties in developing fragility curves. [12] applied the PBPD methodology to the same type of CBFs, and the results revealed that frames designed with this approach exhibit better performance and reduced vulnerability on fragility curves compared to those designed according to current methodologies on seismic codes. [13] expanded on [12] by developing fragility curves using experimental data that simulated real boundary conditions and inelastic responses and compared these curves for CBFs designed with an improved design procedure to those based on standard methods. Recent research examined the seismic performance of low-to-mid-rise steel frames with inverted V-bracing, using fragility curves and a non-linear pushover method in the SeismoStruct program to generate a capacity spectrum. [14] did study that analyzed the seismic behavior of knee-braced steel frames using nonlinear static and dynamic methods to create fragility curves. Four knee brace designs at different heights were modeled in ETABS and PERFORM 3D, and

DOI: https://doi.org/10.11113/jurnalteknologi.v88.26026

seismic parameters were compared through pushover analysis with five far-fault and five near-fault records. [15] A recent study investigates the in-plane (IP) and out-of-plane (OOP) collapse of unreinforced masonry infills (MIs) in hospitals retrofitted with hysteretic damped braces (HYDBs). Using a five-story hospital pavilion in Italy as a case study, nonlinear time-history analyses demonstrate that HYDBs effectively prevent IP and OOP failures of MIs at the Serviceability Design Earthquake (SDE) level without compromising safety during the Maximum Considered Earthquake (MCE). [16]. A study on reinforced concrete special moment frames found that including infill walls increases stiffness and ultimate strength but decreases ductility and energy absorption. Infill walls suffered significant damage, leading to strength loss, and aftershocks amplified structural responses by 20-100%, emphasizing the need to account for aftershocks in design [17].

The interaction of infill walls within braced frame systems has been insufficiently explored in prior research. A notable gap in the previous research is the lack of fragility curve development for concentric braced frames and their interaction with infill walls, which this study seeks to address. Accordingly, the objectives of this study were threefold. First, the research aimed to investigate the influence of infill walls on the failure mechanisms of Chevron-braced and X-braced frames. Second, it sought to quantify the inter-story drift demands and capacities of these braced systems, both with and without the contribution of infill walls, to evaluate their seismic performance under varying structural configurations. Third, the study aimed to develop seismic fragility curves for Chevron- and X-braced frames while explicitly considering the presence or absence of infill–frame interaction. Together, these objectives address key gaps in understanding how infill walls modify the seismic behavior of concentrically braced frames and contribute to more accurate performance-based assessment.

2.0 METHODOLOGY

2.1 SELECTION AND DESIGN OF REFERENCE FRAMES

Twelve steel frames featuring chevron and X bracing were selected for analysis. These frames encompassed six different arrangements, ranging from two- to seven-story configurations, with a specific focus on assessing the impact of infill walls. The ground floor maintained a height of 4 meters, while each successive floor had a height of 3 meters. There were two structural frameworks for each braced frame configuration. For the chevron-braced frame, the structural framework consisted of three bays, with each bay measuring 5 meters in length and incorporating chevron bracing in the central bay. For the X-braced frame, the structural framework consisted of three bays, with each bay measuring 6 meters in length and incorporating X bracing in the central bay. The assumed connections included pin connections between columns and beams, while the connection between columns and the foundation was assumed to be fixed. The analysis and simulation of these structural configurations were conducted using SAP2000 v25 software. The frames underwent a gravity load analysis and were designed in accordance with Eurocode 3. A dead load of 5 kN/m² was applied, with live loads for inter-story levels and the roof set at 2 kN/m², following Eurocode 1 guidelines. The walls, each having a width of 10 cm and concrete mortar with a thickness of 20 cm on both faces (total of 40 cm), were considered. The weights of the brick and concrete mortar were taken as 18.5 kN/m² and 21 kN/m² respectively. For the seismic analysis, Eurocode 8 was applied. Subsequently, a 2D frame analysis was conducted to assess the structural response under both gravitational and seismic conditions, following the extraction of an elevation view of the model. Several key parameters considered in this framework were listed in Tables 1 and 2.

Table 1 Total loads on the frames.

Parameters	Chevron Braced Frame	X Braced Frame
Gravity Load	12.5 kN/m	25 kN/m
Bricks Weight	5.55 kN/m	5.55 kN/m
Weight of concrete mortar	2.52 kN/m	2.52 kN/m
Total D.L.	20.57 kN/m	33.07 kN/m
Total L.L.	5kN/m	10 kN/m

The tributary widths of 2.5 m and 5 m were assigned to the Chevron and X-braced frames, respectively, to represent the portion of the floor load carried by each frame line according to the bay configuration. These tributary widths were used to calculate the live load of 2 kN/m² and the gravity load. The gravity load was subsequently combined with the weights of the brick infill and concrete mortar to obtain the total dead load value.

Table 2 Other Parameters on the frames.

Parameters	Chevron Braced Frame	X Braced Frame
Soil Type	Stiff Soil, Type A	
Ground Acceleration	0.2g	0.3g
Response Spectrum	Type 2 Eurocode 8	
Section Characteristics	H-sections for columns I-sections for beams tube sections for braces	

Multiple plastic hinges were assigned to both structural and non-structural elements in all frames, one flexural hinge was assigned at the middle of

DOI: https://doi.org/10.11113/jurnalteknologi.v88.26026

each beam, one axial hinge was assigned at the middle of each brace and two PMM (axial force and biaxial bending moment) hinges were assigned at both ends of each column. The section geometry of the infill wall is found by employing the equivalent strut approach, which entails substituting the infill wall with a diagonal strut that possesses a breadth equivalent to one-third of the diagonal strut. This method guarantees the integration of precise and standardized section attributes for the subsequent structural analysis. For infill walls plastic hinge properties were defined as shown in table 3, and one plastic hinge was assigned at the mid-length of each wall. For acceptance criteria for Plastic Displacement of hinge parameters across different damage states will be shown in table 4.

Table 3 Plastic hinges parameters and properties for infill walls.

Point	Disp/SF	Force/SF
E-	-12.5	-9450
D-	-12.4	-9450
C-	-1.1	-118125
B-	0	-94500
A	0	0
B	0	94500
C	1.1	118125
D	12.4	9450
E	12.5	9450

Table 4 Acceptance criteria for PDisp/SF of hinge parameters across different damage states.

	Acceptance criteria (Plastic Disp/SF)
IO	1
LS	5
CP	8

When designing braced frames with Chevron braces, it is essential to consider the unbalanced forces resulting from the differential behavior of the compression and tension braces. Under lateral loads, one brace in the Chevron configuration typically experiences compression while the other undergoes tension. This difference in behavior generates a vertical component of force at the connection point where the braces meet the beam. The beam must resist this vertical force, placing additional demands on the beam and its connections which involve increasing the beam's size. Figure 2 from [18] illustrates the unbalanced force equation.

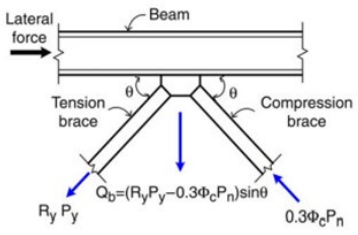


Figure 2 Unbalanced force due to buckling of compression braces. [18]

For this reason, the study increased the size of the middle beams that have Chevron braces (mid-bay of the frame) after calculating the unbalanced forces resulting from the differential behavior of the compression and tension braces. This ensures that these beams will be able to resist the vertical forces effectively.

2.2 MEMBER SELECTION BASED ON ANALYSIS RESULTS

Upon assigning all loads, SAP2000 evaluates the adequacy of the frame by analyzing the applied forces, as well as the shear and moment from the structural analysis. Achieving an optimal design requires assessing the demand-to-capacity (D/C) ratio for each structural component. The target D/C ratio is between 0.3 and 1, except for middle beams with Chevron braces located in the mid-bay of the frame. The sizes of these beams are increased to account for unbalanced forces, ensuring they can effectively resist dead and live loads. This adjustment reduces the D/C ratio for the beams but increases it for the braces supporting them due to the redistribution of forces. Generally, maintaining this range prevents excessive over-design while safeguarding against structural failure. When the D/C ratio falls below 0.3 or exceeds 1, modifications are made to maintain structural integrity by decreasing or increasing the size of the affected elements. In the software, the infill walls, referred to as "bricks," have a uniform size of 1000 mm × 100 mm for all frames in which they are incorporated, as previously mentioned.

2.3 SELECTION OF GROUND ACCELERATION AND EARTHQUAKE RECORDS

The simulated records are generated by modeling seismological sources, whereas natural records come from real seismic events. Due to the ease of online access to natural earthquake databases, these records have become more popular and promising for seismic analysis. [19]

Researchers and design standards have proposed various methods for selecting appropriate earthquake records. The soil profile plays a crucial role in influencing the amplitude and response spectra of earthquake records, making it an essential factor in record selection. It is important to emphasize that when considering the soil profile, the site classification must be determined with a high degree of certainty. Before being used incremental dynamic analysis (IDA) to evaluate the seismic demand or capacity of structures, selected earthquake records must be scaled to multiple intensity levels. Several methods can be employed for scaling earthquake records.

In this study, IDA was performed using 15 natural earthquake records from both near-field and far-field

DOI: https://doi.org/10.11113/jurnalteknologi.v88.26026

events, all recorded on stiff soil classified as type A. Table 5 provides a detailed overview of these records, which have durations ranging from 15 to 35 seconds. Additionally, the selected records exhibit peak ground acceleration (PGA) to peak ground velocity (PGV) ratios ranging between 0.05 and 1 g/m/s. Research has shown that the PGA/PGV ratio of earthquake records can reflect their relative frequency content and duration, significantly influencing the peak inelastic response. [20]

The study obtained time history graphs from the software; these records were defined in SAP2000 as time history functions. This procedure has been applied exclusively to the time history non-linear load cases analysis.

Table 5 Data of the earthquake records.

No	Name	Date of occ.	P. Acc.	P. Vel.	Rec. dur.
1	LBE, CN51W	1933	95.63	-23.68	30
2	LBE, CN39E	1933	62.32	-17.34	30
3	LCECS00W	1934	-156.82	-20.85	25
4	SFECN61W	1971	98.74	19.30	20
5	IVECS00E	1940	341.70	33.44	30
6	KCCES69E	1952	175.94	-17.72	25
7	KCCEN21E	1952	152.70	-15.72	25
8	BMECN57W	1968	-45.53	-4.20	35
9	MN2E	1979	0.17	0.19	20
10	BL3E	1981	0.07	0.03	10
11	PE	1966	-425.67	-25.45	15
12	SFECS09E	1957	-83.80	-5.05	35
13	SFECS74W	1971	1054.94	-57.74	15
14	SFECS21W	1971	-143.50	-8.53	20
15	SFECS98W	1973	-200.9	27.5	35

2.4 NONLINEAR FINITE ELEMENT MODELS WITH LOAD PATTERN AND CASES OF FRAMES

In this study, we employed the lumped plastic model to simulate the inelastic seismic response of various structural components, including beams, columns, chevron-braced frames, and infill walls. This modeling approach involved the allocation of plastic hinges at both ends of the beams and columns, as well as at the centers of the braces and infill walls, to capture their inelastic behavior. The moment–rotation response of these plastic hinges was determined based on the relevant mechanical properties and the recommendations provided by [21]. The structural framework was assessed under two conditions: first, accounting for the effect of infill walls—considering their strength, stiffness, and weight—and second, excluding the effect of infill walls, with only their weight taken into consideration. To analyze and construct the numerically simulated models, it was essential to define multiple load cases to which the structure would be subjected during analysis. The gravity load case was designated as a linear static analysis, incorporating both dead and live loads, with a scale factor of 1 for the dead load and 0.25 for the live load, based on Eurocode provisions. Subsequently, the "push uniform" and "push first mode" load cases were established as nonlinear static analyses, with the load type set to acceleration and a scale factor of 1. Additionally, multiple load cases were defined based on the time-history analysis of 15 earthquake records. These were characterized as nonlinear direct-integration history analyses, with scale factors determined by the intensity or peak ground acceleration (PGA) values ranging from 0.05 to 0.5, multiplied by the acceleration due to gravity (9.81 m/s²).

Subsequently, the study defined the drift displacement between each storey in all frames by using the "Define Generalized Displacement" function in SAP2000. This involved taking 33% of the displacement from each joint and subtracting 33% of the subsequent displacement. This method allowed for the definition of a plot function to display the Inter-Storey drift values resulting from all load cases.

2.5 INTER STORY DRIFT DEMAND AND CAPACITY

Inter-story drift demand entails the simulation of 15 earthquake records spanning various intensities (0.05g to 0.5g) to evaluate drift levels under each intensity. Conversely, Inter-story drift capacity necessitates simulating these records to assess drift during specific damage states only, namely Immediate Occupancy (IO), Life Safety (LS), and Collapse Prevention (CP). Following the allocation of plastic hinges within the frames and the subsequent simulation of 15 earthquake records ranging in intensity from 0.05g to 0.5g, the median and standard deviation values for inter-story drift demand for both chevron- and X-braced frames, with and without infill walls, were computed and building on this, the median and average values for inter-story drift capacity were then computed to assess drift levels corresponding to specific damage states (IO, LS, and CP) for chevron- and X-braced frames, with and without infill walls.

2.6 ANALYTICAL DERIVATION OF SEISMIC FRAGILITY CURVES

DOI: https://doi.org/10.11113/jurnalteknologi.v88.26026

Fragility curves were analytically derived to provide essential damage data, enhance seismic assessment accuracy, and enable precise predictions of potential earthquake-induced damage. These curves represented a fundamental tool for quantifying the seismic risk associated with structurally vulnerable buildings, serving as benchmarks for gauging the extent of damage in these deficient structures. [22] developed probabilistic equations, as shown in equation 1, to derive fragility curves.

$$P(DS:SI) = 1 - \Phi\left(\frac{\lambda_c - \lambda_{d:SI}}{\sqrt{\beta_{D:SI}{}^2 + \beta_c{}^2 + \beta_M{}^2}}\right)$$

$$\beta_{D:SI} = \sqrt{\ln(1+S^2)}$$

$$\beta_c = \sqrt{\ln(1+Cov^2)}$$

Equation 1 Probabilistic equations for derivation of fragility curves. [22]

Where, P(DS:SI) Is conditional probability of exceeding a DS for a given SI, Φ Is standard normal distribution, λ_c Is Natural Log of median drift capacity of DS, $\lambda_{d:SI}$ Natural Log of computed median drift demand given SI, S^2, Is standard error, Cov Is coefficient of variance, βD:SI Is demand uncertainties based on SI and βc & βm Are uncertainties of capacity and modelling respectively. [22].

3.0 RESULTS AND DISCUSSION

3.1 PUSHOVER ANALYSIS FOR REFERENCE FRAMES

The examination delved into the failure mechanisms of concentric-braced frames, with and without infill walls, through an assessment of the positioning of plastic hinge formation and the extent of damage evident at each plastic hinge. The structural frame was subjected to analysis under two distinct load distribution scenarios: one involving a lateral load uniformly distributed across all floors, and another involving a lateral load pattern conforming to the deformed shape of the first mode, as prescribed by [21]. The emergence of plastic hinges, as derived from the pushover analysis of Chevron and X-braced frames with and without infill walls, was elaborated upon in Tables 6 and 7.

Table 6 Plastic hinges for chevron braced frames, (Displacement in mm).

PUSH OVER	PUSH UNIFORM				PUSH FIRST MODE			
Num. Stor.	Dam. State	IO	LS	CP	Dam. State	IO	LS	CP
3-WOI	Disp.	6.3	28	34	Disp.	7.9	33	42
	hinges	1	1	1	hinges	2	1	1
3-WI	Disp.	3.4	15	18	Disp.	4	18	21
	hinges	1	1	1	hinges	1	1	1
5-WOI	Disp.	7.8	34	54	Disp.	30	48	-
	hinges	1	1	2	hinges	4	4	-
5-WI	Disp.	4.3	20	23	Disp.	18	24	47
	hinges	1	1	1	hinges	6	1	6
7WOI	Disp.	9.6	41	-	Disp.	16	38	48.
	hinges	1	1	-	hinges	3	2	1
7-WI	Disp.	4.6	20	24	Disp.	5.4	23	27
	hinges	1	1	1	hinges	3	1	1

For chevron-braced frames, the presence of infill walls in the frame leads to an earlier commencement of failure in comparison to the frame without infill walls. Furthermore, it is evident that the frame with infill walls necessitates a notably reduced displacement to achieve the Collapse Prevention (CP) state, suggesting an earlier onset of damage for the braced frames with infill walls compared to its counterpart lacking infill walls.

Table 7 Plastic hinges for X-braced frames, (Displacement in mm).

PUSH OVER	PUSH UNIFORM				PUSH FIRST MODE			
Num. Stor.	Damage State	IO	LS	CP	Damage State	IO	LS	CP
2-WOI	Disp.	18	-	49	Disp.	20	-	-
	hinges	2	-	1	hinges	2	-	-
2-WI	Disp.	20	22	29	Disp.	23	25	32
	hinges	2	1	1	hinges	2	1	1
4-WOI	Disp.	36	-	70	Disp.	18	78	99
	hinges	4	-	1	hinges	1	2	2
4-WI	Disp.	36	-	-	Disp.	31	-	-
	hinges	4	-	-	hinges	4	-	-
6WOI	Disp.	57	-	89	Disp.	30	77	-
	hinges	6	-	1	hinges	2	1	-
6-WI	Disp.	35	-	-	Disp.	30	-	-
	hinges	3	-	-	hinges	2	-	-

For the X-braced frames, the two-story configuration with an infill exhibited noticeably earlier deterioration compared to its counterpart without an infill. Rather than simply accelerating the onset of damage, the presence of the infill appeared to alter the overall deformation pattern, leading the system to reach the Collapse Prevention (CP) limit state at substantially lower displacements. This suggests that, in low-rise frames, the increased stiffness introduced by the infill may concentrate demands prematurely, reducing the deformation capacity of the bracing system. In contrast, the four- and six-story frames without infill walls entered the Immediate Occupancy (IO) state earlier due to their relatively lower stiffness; however,

DOI: https://doi.org/10.11113/jurnalteknologi.v88.26026

they continued to transition through Life Safety (LS) and CP states in a more gradual manner. The corresponding frames with infill did not reach LS or CP within the examined displacement range, indicating that the infill contributed not only to stiffness but also to a redistribution of lateral demands that delayed higher-level damage. This divergence in behavior highlights that the influence of infill walls is not uniform across building heights: while they can be detrimental for short frames by accelerating failure mechanisms, they tend to enhance the deformation capacity and delay severe damage in taller configurations.

3.2 INTER STORY DRIFT

Inter-story drift demand and capacity are critical for assessing the structural performance and integrity of buildings, as excessive inter-story drift can lead to structural damage or even collapse. They are typically expressed as the maximum allowable horizontal displacement or drift angle between consecutive floors of a multi-story structure under seismic loading conditions before structural damage or failure occurs and are used to evaluate the adequacy of structural design and the effectiveness of seismic retrofit measures in mitigating seismic risks. The distinction between Inter-story drift capacity and Inter-story drift demand lies in their respective assessment methodologies. These values are depicted in Tables 8&9.

Table 8 Inter story drift Capacity for chevron braced frames.

Num. Stories	Damage State	IO	LS	CP
3-WOI	Median	0.00096	0.00370	0.0049
	Average	0.00096	0.00359	0.0049
3-WI	Median	0.00042	0.00133	0.0017
	Average	0.00042	0.00135	0.0019
5-WOI	Median	0.00118	0.00425	0.0047
	Average	0.00115	0.00414	0.0049
5-WI	Median	0.00052	0.00209	0.0027
	Average	0.00050	0.00205	0.0027
7WOI	Median	0.00151	0.00520	0.0067
	Average	0.00158	0.00494	0.0066
7-WI	Median	0.00051	0.00164	0.0020
	Average	0.00054	0.00169	0.0020

Table 9 Inter story drift Capacity for X braced frames.

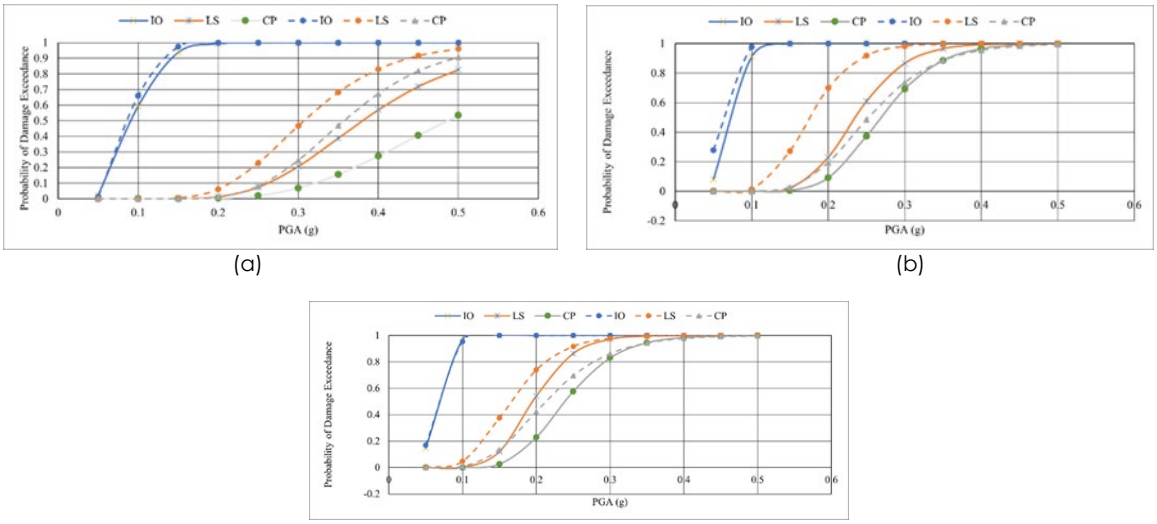
Num. Stories	Damage State	IO	LS	CP
2IWOI	Median	0.00050	0.00126	0.0018
	Average	0.00052	0.00161	0.0024
2-WI	Median	0.00079	0.00314	0.0039
	Average	0.00076	0.00271	0.0039
4-WOI	Median	0.00144	0.00521	0.0070
	Average	0.00121	0.00496	0.0061
4-WI	Median	0.00100	0.00195	0.0060
	Average	0.00106	0.00334	0.0052
6-WOI	Median	0.00337	0.01070	0.0164
	Average	0.00335	0.01163	0.0177
6-WI	Median	0.00147	0.00276	0.0035
	Average	0.00139	0.00327	0.0043

The observation indicates a direct correlation between drift demands and increasing Peak Ground Acceleration (PGA). The observation indicates a proportional increase in drift demands with increasing PGAs. For drift capacity, median and average calculated based on all damage states (IO, LS, and CP). As observed, chevron braced frames without an infill wall exhibit a broader range of median drift demand values and necessitate a higher drift displacement to transition from IO to CP compared to the frames with an infill wall. This higher median drift demand and elevated median drift capacity implies a more substantial lateral displacement between adjacent stories under seismic loading conditions. For X braced frames, the observed damage is concentrated predominantly at the first story for two-story frames, while for four and six-story frames, the initial damage state is more prominently observed at higher stories. This discernment underscores the nuanced dynamics influencing inter-story drift capacity across different structural configurations.

3.3 FRAGILITY CURVES GRAPHS

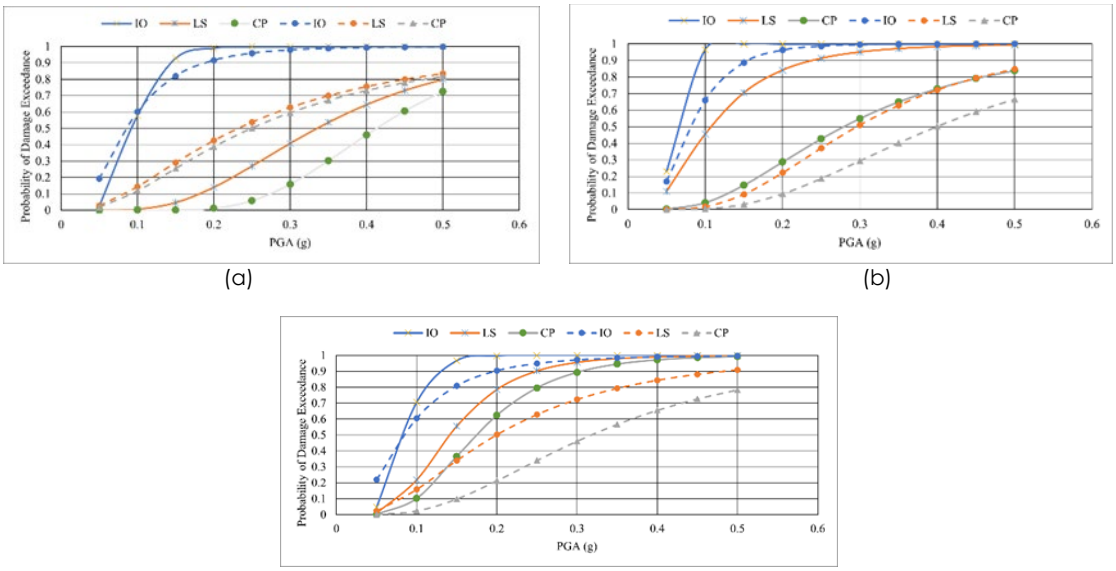
Fragility curves were derived to enhance the accuracy of seismic assessment and to predict earthquake-induced damage using the probabilistic equations developed by [22]. These curves were essential for quantifying seismic risk in structurally vulnerable buildings and served as benchmarks for evaluating damage in deficient structures. The graphs presented in Figures 4 and 5 show the fragility curves for Chevron- and X-braced frames, with and without infill walls, calculated using the relevant parameters and a series of incremental Peak Ground Accelerations (PGAs). The solid lines represented the Chevron- and X-braced frames with infill walls, whereas the dashed lines denoted the corresponding frames without infill walls.

DOI: https://doi.org/10.11113/jurnalteknologi.v88.26026



(a) (b) (c)

Figure 4 Fragility Curves graphs for chevron braced frames with and without Infill Wall (a) Three-storey frames, (b) Five-storey frames, (c) Seven-storey frames.



(a) (b) (c)

Figure 5 Fragility Curves graphs for X braced frames with and without Infill Wall (a) Two-storey frames, (b) Four-storey frames, (c) Six-storey frames.

For the Chevron-braced frame, the probabilities of exceeding the IO, LS, and CP damage states for the frame without an infill wall were higher than those for the frame with an infill wall by 37.25%, 0.4%, and 0.27%, respectively, at a PGA of 0.2g. This indicates that the progression from the IO to the CP damage state occurred more rapidly in the absence of an infill wall, demonstrating that Chevron-braced frames without infill walls are more susceptible to earthquake-induced damage.

For the X-braced frame, the statistical analysis showed that at a PGA of 0.1g, the probability of exceeding the Immediate Occupancy (IO) damage state was higher for all frames without infill walls compared to the frame with an infill wall. However, at PGA levels greater than 0.1g, the probability of exceeding each damage state became lower for the frames without infill walls relative to the frame with an infill wall.

DOI: https://doi.org/10.11113/jurnalteknologi.v88.26026

4.0 CONCLUSION

This study demonstrates that the seismic response of concentrically braced frames is highly dependent on both the presence of infill walls and the number of stories. For X-braced frames, infill walls contribute to earlier attainment of collapse-related performance limits in low-rise configurations, whereas in mid- and high-rise frames they tend to improve overall seismic performance at higher ground-motion intensities. In Chevron-braced systems, infill walls generally reduce drift capacity, while bare frames exhibit greater capacity but a more rapid progression through damage states. The fragility results reinforce that infill walls can either mitigate or exacerbate seismic vulnerability depending on structural height. Collectively, the findings highlight that infill–frame interaction plays a decisive role in modifying stiffness, drift demand, and failure likelihood, underscoring the need to explicitly account for story height and infill configuration in the seismic design and evaluation of braced frames.

5.0 RECOMMENDATIONS

Future research could broaden the scope of the present work by examining additional configurations of concentric bracing, including diagonal and eccentric systems, to enable more comprehensive comparative assessments. Beyond the building heights considered here, extending the analysis to structures with a wider range of story numbers would help clarify height-dependent seismic behaviors. Increasing the number of ground-motion records used in simulations would further strengthen the statistical robustness and reliability of seismic demand estimates. Moreover, incorporating frames with low and medium ductility levels, rather than assuming only highly ductile behavior, would provide a more complete understanding of performance across different detailing practices. Finally, as this study is limited to structures founded on stiff soil, future investigations should consider a broader spectrum of soil conditions to more accurately capture the influence of site characteristics on seismic response.

Acknowledgement

This research was funded by the UTM Fundamental Research Grant (PY/2024/01221, Cost Centre No. Q.J130000.3822.23H73), which is gratefully acknowledged. The dissemination of this work was made possible through additional financial support from Budapest University of Technology and Economics (BME) and Malaysian Ministry of Foreign Affairs through the Malaysian Technical Cooperation Programme (MTCP) Scholarship (No. KLN.600-4/91/70 2022).

Conflict of Interest

The authors declare they have no financial interests.

Author Contributions Statement

All authors reviewed the manuscript.

Data Availability Statement

Data will be made available on reasonable request.

References

[1] R. A. Jazany, I. Hajirasouliha, and H. Farshchi, "Influence of masonry infill on the seismic performance of concentrically braced frames," J Constr Steel Res, Vol. 88, pp. 150–163, 2013, doi: 10.1016/j.jcsr.2013.05.009.
[2] D. G. Lignos and E. Karamanci, "Drift-based and dual-parameter fragility curves for concentrically braced frames in seismic regions," J Constr Steel Res, Vol. 90, pp. 209–220, 2013, doi: 10.1016/j.jcsr.2013.07.034.
[3] M. Hassan, N. Sipcic, and G. Vasdravellis, "Seismic performance evaluation of high-post-yield stiffness concentrically braced steel frames under mainshock-consistent-aftershock sequences," Earthq Eng Struct Dyn, Vol. 52, No. 7, pp. 2222–2250, Jun. 2023, doi: 10.1002/EQE.3880.
[4] Ali Mohammadgholipour and AHM Muntasir Billah, "Performance-based plastic design and seismic fragility assessment for chevron braced steel frames considering aftershock effects," Soil Dynamics and Earthquake Engineering, Vol. 178, Mar. 2024.
[5] Adil Emre Özel and Esra Mete Güneyisi, "Effects of eccentric steel bracing systems on seismic fragility curves of mid-rise R/C buildings: A case study," Structural Safety, Vol. 33, No. 1, pp. 82–95, Jan. 2011.
[6] Cheng Fang, Boyan Ping, Yue Zheng, Yiwei Ping, and Hao Ling, "Seismic fragility and loss estimation of self-centering steel braced frames under mainshock-aftershock sequences," Journal of Building Engineering, Vol. 73, Aug. 2023.
[7] Muhammad Shoaib Khan, Abdul Basit, Muhammad Rizwan, and Naveed Ahmad, "Seismic fragility functions for RC As-built and eccentric steel brace frames," Structures, Vol. 50, pp. 1338–1352, Apr. 2023.
[8] Mojtaba Gorji Azandariani, Ali Gorji Azandariani, Ali Mohammad Rousta, and Hamid Malek Nia, "Seismic fragility assessment of reinforced concrete moment frames retrofitted with strongback braced system," Results in Engineering, Vol. 20, Dec. 2023.
[9] Maryam Behrangfar, Mohsen Gerami, and Mehrsa Mirzahosseini, "The effect of the ground motion frequency content on seismic performance and fragility curve of special concentric braced frames," Structures, Vol. 57, Nov. 2023.
[10] Mahmoud Faytarouni, Onur Seker, Bulent Akbas, and Jay Shen, "Seismic assessment of ductile concentrically braced frames with HSS bracings," Eng Struct, Vol. 191, pp. 401–416, Jul. 2019.
[11] Dimitrios G. Lignos and Emre Karamanci, "Drift-based and dual-parameter fragility curves for concentrically braced frames in seismic regions," J Constr Steel Res, Vol. 90, pp. 209–220, Nov. 2013.

DOI: https://doi.org/10.11113/jurnalteknologi.v88.26026

[12] M.R. Banihashemi, A.R. Mirzagoltabar, and H.R. Tavakoli, "Reliability and fragility curve assessment of steel concentrically braced frames," European Journal of Environmental and Civil Engineering, Vol. 20, No. 7, pp. 748–770, Jul. 2016.
[13] Charles W. Roeder, Eric J. Lumpkin, and Dawn E. Lehman, "Seismic Performance Assessment of Concentrically Braced Steel Frames," Earthquake Spectra, Vol. 28, No. 2, May 2012.
[14] Pramesta Praba Sumedi, Senot Sangadji, and Halwan Alfisa Saifullah, "The fragility curve of low-to-mid-rise steel frame buildings retrofitted with inverted V-bracing ," AIP Conf Proc, Vol. 2696, No. 1, Aug. 2023.
[15] R. Yahyapour and S. M. Seyedpoor, "Comparing the Seismic Behavior of Various Knee Braced Steel Frames Based on Incremental Dynamic Analysis and Development of Fragility Curves," International Journal of Steel Structures, Vol. 21, pp. 1228–1241, Jun. 2021.
[16] F. Mazza, "In-plane and out-of-plane nonlinear seismic response of masonry infills for hospitals retrofitted with hysteretic damped braces," Soil Dynamics and Earthquake Engineering, Vol. 148, Sep. 2021, doi: 10.1016/j.soildyn.2021.106803.
[17] A. Jalaeefar and A. Zargar, "Effect of infill walls on behavior of reinforced concrete special moment frames under seismic sequences," Structures, Vol. 28, pp. 766–773, Dec. 2020, doi: 10.1016/j.istruc.2020.09.029.
[18] Jinkoo Kim and Hyunhoon Choi, "Response modification factors of chevron-braced frames," Eng Struct, Vol. 27, Dec. 2004.
[19] Nicola Caterino, Iunio Iervolino, Gaetano Manfredi, and Edoardo Cosenza, "Multi-Criteria Decision Making for Seismic Retrofitting of RC Structures," Journal of Earthquake Engineering, Vol. 12, No. 4, May 2008.
[20] W. K. Tso, T. J. Zhu, and A. C. Heidebrecht, "Engineering implication of ground motion A/V ratio," 1992.
[21] Seismic Evaluation and Retrofit of Existing Buildings. Reston, VA: American Society of Civil Engineers, 2017. DOI:10.1061/9780784414859.
[22] M. E. and B. R. E. M. E. Y. K. Wen, "The Role of Fragility Assessment in Consequence-Based Engineering," Saga Journal, Vol. 21, No. 3, Aug. 2005.